SOLAR HARD X-RAY AND GAMMA-RAY OBSERVATIONS FROM *GRANAT*[1]

N. VILMER[2]
DASOP—Observatoire de Paris, Section d'Astrophysique de Meudon, F92195 Meudon-Cedex, France

ABSTRACT

Hard X-rays and gamma-rays are the most direct signature of the energetic electrons and ions which are accelerated during solar flares. Since the beginning of 1990 the PHEBUS instrument and the SIGMA anticoincidence shield aboard GRANAT have provided hard X-ray and gamma-ray observations of solar bursts in the energy range 0.075–124 and 0.200–15 MeV, respectively. After a brief description of the experiments, we present some results obtained on solar bursts recorded in 1990 and 1991 June. Special emphasis is given to the results related with particle acceleration during solar flares.

The first part of the review is devoted to the constraints obtained on the electron acceleration timescale through the analysis of the temporal characteristics of the bursts. Combined studies of hard X-ray and gamma-ray emissions from PHEBUS and radio emissions from the Nançay Multifrequency Radioheliograph are used to infer constraints on the coronal magnetic topology involved in flares. The characteristics (location, spectrum) of the radio-emitting sources are found to vary within a flare from one hard X-ray peak to the other. Hard X-ray and gamma-ray burst onsets and rapid increases of the >10 MeV emission are coincident with changes in the associated radio emission pattern. These results will be discussed in the context of the flare energy release.

The second part of the paper concerns the heliocentric angle distribution of >10 MeV events and presents more detailed observations of some of the largest flares in the gamma-ray line and the high-energy domains produced by ultrarelativistic electrons and >100 MeV nucleon^{-1} ions. The PHEBUS observations of the gamma-ray line flare of 11 June 1991 have been used to deduce the hardness of the accelerated ion spectrum. The link between the main part of the flare and the late long-lasting >50 MeV emission detected by EGRET/COMPTON is discussed. Finally some observations of the large 1990 May 24 flare which produced a large neutron event at ground level are presented.

Subject headings: acceleration of particles — Sun: flares — Sun: radio radiation — Sun: X-rays, gamma rays

1. INTRODUCTION

Particles accelerated during solar flares have now been detected and studied for several decades through first ground-based then satellite-borne observations. The knowledge of the characteristics of these accelerated particles (number, spectrum) is crucial for the understanding of solar flares since a large fraction of the energy released is transferred to these particles. They are detected either in the interplanetary space or through the radiation that they produce when interacting at the Sun. This paper concerns the most direct diagnostic of the particles interacting at the Sun: hard X-ray and gamma-ray emissions. To a lesser extent, we shall also discuss some additional radio observations which provide complementary constraints on the coronal magnetic topology in which energetic particles propagate from the acceleration site.

Many theoretical studies have given a detailed description of the components of the solar gamma-ray spectrum expected from flare-accelerated ions interacting with the solar atmosphere (see, e.g., Ramaty & Murphy 1987 for a review). Since the first detection of solar gamma-ray lines by OSO7 and Prognoz (Chupp et al. 1973; Talon et al. 1975), many gamma-ray line spectra have been obtained with the spectrometers aboard

SMM (see, e.g., Chupp 1990a; Rieger 1990 for reviews), *Hinotori* (Yoshimori 1989), and more recently *COMPTON* (Murphy et al. 1993) and *YOHKOH* (Yoshimori et al. 1992). A typical gamma-ray spectrum consists of several prompt nuclear de-excitation lines from elements of the solar atmosphere (e.g., Fe, Mg, Ne, Si, C, O) and of some delayed lines such as the neutron radiative capture line at 2.223 MeV. This gamma-ray line spectrum is superposed on a continuum made of the same kinetically broadened de-excitation lines and of a bremsstrahlung component extending above 1 MeV. For a fraction of events, this last component has been detected above 10 MeV (10% of the flares detected from 1980 to 1989) (see, e.g., Vestrand, Forrest, & Rieger 1991) and for an even smaller number of events up to a few hundred MeV (Akimov et al. 1991; Leikov et al. 1993; Kanbach et al. 1993). The gamma-ray lines are produced by nuclear reactions of energetic ions (typically in the 10–100 MeV nucleon^{-1} range) impinging on the solar atmosphere. These reactions result in excited nuclei with short lifetimes ($<10^{-11}$ s) producing the de-excitation "prompt" gamma-ray lines and in secondary products such as pions (for protons >200 MeV) and neutrons. These secondary products give rise respectively to an additional large band contribution essentially at energies above 10 MeV (with a broad peak around 70 MeV) and to the delayed 2.223 MeV line (see, e.g., Ramaty & Murphy 1987 for a review). If the spectrum of accelerated ions extends above a few hundred MeV nucleons^{-1}, the energetic neutrons produced in nuclear reactions

---

can also be directly detected in the interplanetary space (>50 MeV neutrons) or at ground level (>200 MeV neutrons) (see, e.g., Chupp 1988 for a review). Although alternative mechanisms have been proposed in the literature (Heristchi 1986), the continuous spectrum of photons above a few tens of keV (>30 keV) is generally attributed to bremsstrahlung emission of nonthermal electrons with energies greater than 30 keV. The nonthermal electron spectrum is well represented by one or two power laws in energy in the 0.01–10 MeV range (see, e.g., Dennis 1988).

Although a complete knowledge of the way in which the Sun accelerates particles still requires refined experimental data, much information on these accelerated particles has been obtained in the last 10 years with the observations of X-ray and gamma-ray spectrometers aboard the *Solar Maximum Mission* (*SMM*) (see, e.g., Chupp 1990a; Rieger 1990 for reviews) and *Hinotori* satellites (Yoshimori 1989). Some of the constraints deduced from these observations on particle acceleration in solar flares are recalled below:

Typical values of the number of nonthermal electrons involved in the production of hard X-ray emission are of the order of 10^{36}–10^{37} electrons above 25 keV for impulsive flares and greater than 10^{38} electrons for long-duration gradual events (Bruggmann et al. 1993). The energy content in the nonthermal electrons (>25 keV) is thus of the order of 10^{30} ergs for impulsive flares up to 10^{31} ergs for gradual ones and represents a large fraction of the total flare energy (Wu et al. 1986; Bruggmann et al. 1993).

Ion acceleration is also observed frequently in flares, but the electron to ion ratio is highly variable (see, e.g., Chupp 1990a). Extreme cases can be found in the observations of "electron-dominated events" which are produced by transient acceleration of electrons to energies >10 MeV in less than 2 s (Rieger & Marschhaüser 1990).

The total numbers of protons inferred from the gamma-ray line observations depend on the abundances in the proton interaction region, but typical values lie in the range of 10^{30}–10^{33} protons above 30 MeV (Ramaty et al. 1993). The proton spectra are generally found to be consistent either with a power-law distribution in kinetic energy with a spectral index $3 < s < 4$ or with a Bessel function resulting from a second-order Fermi acceleration process with $0.01 < \alpha T < 0.04$ (where α is the acceleration efficiency and T the particle escaping time from the acceleration region) (see, e.g., Hua & Lingenfelter 1987a). The energy content in >30 MeV protons is thus in the range of 10^{26}–10^{29} ergs.

Fast time structures of a few hundreds of milliseconds in the hard X-ray emission characteristic of the interaction of 100 keV electrons have occasionally been reported (Hurley et al. 1983; Desai et al. 1987). In most events however, energetic electrons (> a few 100 keV) and ions (10–100 MeV nucleon^{-1}) are found to be accelerated together in time scales of 1 s (see, e.g., Kane et al. 1986). Relativistic electrons (10–100 MeV) and >100 MeV nucleon^{-1} ions are rather produced on timescales less than a few tens of seconds at the beginning of a flare (see, e.g., Chupp 1982).

The interaction region for energetic particles is generally located in the dense atmosphere (at least for impulsive flares) (see, e.g., Ramaty & Murphy 1987). However, in some events,

GeV ions are produced or stored in the corona for durations larger than 20 minutes (see, e.g., Forrest et al. 1985).

Since the end of the *Solar Maximum Mission* observation, the PHEBUS instrument and the anticoincidence shield of the SIGMA telescope aboard *GRANAT* have provided observations of solar X-ray and gamma-ray bursts in the energy range 0.075–124 MeV and 0.200–15 MeV, respectively. These observations are the only solar high-energy ones from 1989 December to 1991 April (launch of COMPTON). This paper presents a review of the results of these experiments with special emphasis on the ones concerning particle acceleration in solar flares. In § 2 the two experiments are briefly described. Section 3 is devoted to the results obtained on the electron acceleration time scale. The link between the evolution of the coronal magnetic structures as revealed by radio emissions and the production of energetic electrons is discussed. In § 4 the heliocentric angle distribution of high-energy emissions is investigated and observations of some of the largest flares of the present cycle are presented. The observations of the gamma-ray line flare of 1991 June 11 have been used to determine the hardness of the ion spectrum. The observation of the 1990 May 24 event which produced solar neutrons is also presented. In § 5 these results are summarized.

2. THE HARD X-RAY/GAMMA-RAY DETECTORS ABOARD GRANAT

Two hard X-ray/gamma-ray spectrometers belong to the scientific payload of the *GRANAT* satellite launched on 1989 December 1: the large anticoincidence shield of the SIGMA telescope (Pelaez et al. 1992) and the PHEBUS experiment (Barat et al. 1988; Talon et al. 1993b).

2.1. The Phebus Instrument

This instrument was almost continuously operating since 1990 January 8. However the mean duty cycle does not exceed 35% because of operational constraints (Talon et al. 1993b). The PHEBUS instrument consists of six independent BGO detectors measuring solar and cosmic hard X-ray/gamma-ray bursts in the nominal energy range 0.075–124 MeV. Each BGO crystal is 78 mm in diameter, 120 mm in height and surrounded by a plastic anticoincidence shield to reject charged particles. The detectors are directed along the six axes of a Cartesian coordinate system in order to obtain a complete field of view. At least two detectors always have the Sun in their field of view. The minimum sensitive area for solar flares is thus 187 cm^2. Depending on the pointing of the SIGMA telescope, a third detector can observe the Sun leading to an unobstructed field of view of 280 cm^2. This experiment has two basic modes of operation:

A waiting mode providing for each detector (1) a continuous time history in the 0.1–1.6 MeV energy range (nominal) with a 64 s time resolution, and (2) two background spectra allowing in flight calibration of the detectors.

A burst mode which is triggered when count rates in the 0.1–1.6 MeV range integrated over a 0.25 and 1 s interval exceed the background level by 8 sigmas. The data used here are (1) a time history of the 0.1–1.6 MeV range recorded during 86.6 s after the burst trigger with a time resolution of 31.25

ms and (2) spectral information. After the trigger, 176 spectra are stored over 116 energy channels in a time-to-spill mode covering the 0.1–124 MeV range. The total duration of this record depends on the burst intensity but generally lasts less than 1 minute. We then record 640 spectra with a 1 s time resolution for the 0.1–10 MeV range covered by 26 energy channels and with a 4 s time resolution for the 10–100 MeV band covered by 14 energy channels.

Since the launch of *GRANAT,* more than 100 solar bursts above 0.1 MeV have been recorded. Although the experiment works on the burst trigger mode described above, a complete description of the temporal behavior of some long-duration events can be obtained with the complementary observations of the SIGMA anticoincidence shield since the two experiments do not necessarily trigger their burst mode at the same time (Talon et al. 1993b; Pelaez et al. 1992).

2.2. *The SIGMA Anticoincidence Shield*

The gamma camera aboard *GRANAT* is actively shielded by an anticoincidence device composed of two lateral shells (8×2400 cm^2) and a bottom shell of CsI (70 cm in diameter) (Pelaez et al. 1992). The lateral shells are equipped electronically to detect solar and cosmic gamma-ray bursts. A burst mode is triggered in case of a rapid increase of the incoming photon flux, and more than 20 solar bursts have been recorded so far. The normal area to the Sun is for one sector 1500 cm^2. Two independent sectors are continuously directed toward the Sun. The sensitivity of one sector for a burst trigger is 2 photons cm^{-2} s^{-1} for an integration time of 0.25 s and 0.7 photons cm^{-2} s^{-1} for an integration time of 2 s. The data used here are the spectral information recorded for 11 minutes after the burst trigger in the 200 keV–15 MeV energy range. For the first minute after trigger, 80 channels of spectra are recorded with an accumulation time of 0.125 s for 5 s, 0.5 s for 25 s, and 1 s for 30 s, respectively. For the following 10 minutes, two kinds of data compression are used providing either 80 channels spectra every 20 seconds or 25 channels spectra between 0.2 and 15 MeV every second.

3. NONTHERMAL ELECTRON ENERGY RELEASE DURING SOLAR FLARES

3.1. *Timescales for Electron Acceleration*

The temporal characteristics of the hard X-ray and gamma-ray continua are generally considered as good indicators of the electron acceleration timescales. Fast time structures are systematically observed in the PHEBUS time profiles of "impulsive" events above 100 keV (total duration above 100 keV less than 5 minutes) (Talon et al. 1993b). They consist of significant spikes with typical durations ranging from 250 to 625 ms. A refined analysis performed on all the "impulsive" events recorded by PHEBUS during the first semester of 1990 has confirmed their existence: the temporal structure is considered as significant when it corresponds to a count-rate enhancement of >3 sigmas above the mean of the count rates measured in the time intervals immediately preceding and following the studied feature (see Talon et al. 1993a for examples). Figure 1 shows the temporal evolution of the count rate observed in the
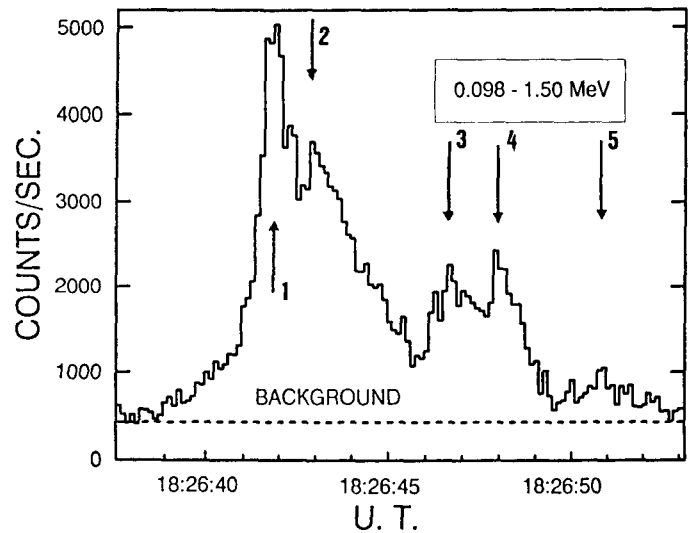

FIG. 1.—From Talon et al. 1993a. Temporal evolution of the count rate observed by PHEBUS above 100 keV with an accumulation time of 125 ms for the 1990 February 11 event. The arrows indicate the five significant peaks (see text).

98 keV–1.5 MeV band for the 1990 February 11 event. The peaks marked 1, 3, and 4 are significant for an accumulation time of 250 ms, while peaks marked 2 and 5 are significant for accumulation times of 375 and 625 ms, respectively (Talon et al. 1993a). The systematic existence of subsecond time structures at energies above 100 keV in "impulsive bursts" must be compared with the previous finding that less than 10% of hard X-ray bursts observed by the HXRBS spectrometer aboard *SMM* exhibit subsecond time structures at energies above 30 keV (Kiplinger et al. 1983). One possible explanation for these different results lies in the fact that the analysis of the HXRBS data was performed at a lower energy (30 keV) where the contribution of the hot thermal plasma is larger. The observations of the 1990 February 11 event with the Konus-B instrument on *GRANAT* support this explanation, since the time profiles recorded in three energy bands between 10 and 750 keV become smoother at lower energies in the deka-keV range (see Fig. 6 of Golonetskii et al. 1991). The other explanation lies in the fact that, while HXRBS data were recorded in a continuous mode, the PHEBUS observations used here are obtained in a burst mode triggered for events with fast rise times (see § 2.1). Such an observing mode could lead to a selection of fast time-varying events. This could be the reason why our results are in agreement with previous occasional reports of subsecond time structures above 100 keV observed also in burst trigger modes (Hurley et al. 1983; Desai et al. 1987) and with recent observations performed in the BATSE and OSSE burst modes triggered in a similar way (Machado et al. 1993; Murphy et al. 1993). These last observations confirm the existence of fine-scale temporal spikes of durations ranging from few tens to several hundreds of milliseconds.

The refined analysis performed on the high-energy impulsive event of 1990 May 11 (Fig. 2) indicates that the four peaks observed in the 7.6–8.6 MeV continuum range during the main phase of the burst (before 20:59 U.T) are significant with
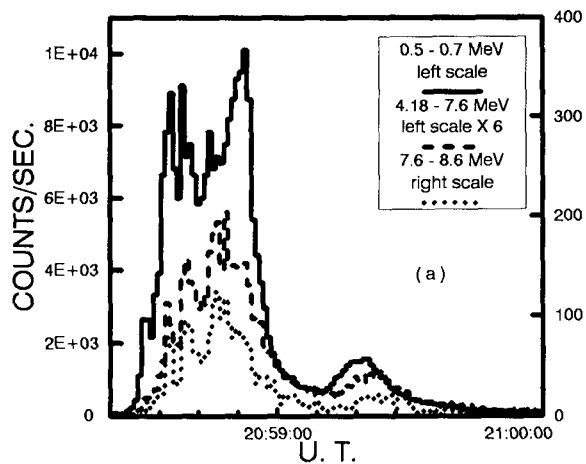
FIG. 2.—From Talon et al. 1993a. Temporal evolution of the count rate observed by PHEBUS with an accumulation time of 1 s during the 1990 May 11 event.

the 1 s time resolution which is the shortest accumulation time available for spectral analysis with the PHEBUS experiment (Talon et al. 1993a). With the large detection area of the SIGMA anticoincidence shield a significant time structure of the order of 1 s is also found for energies as high as 10 MeV for the 1990 June 11 event (Fig. 3) in which the high-energy emission is predominantly radiated by ultrarelativistic electrons (Talon et al. 1993b). The detection of time structures less or of the order of the second up to MeV energies confirms that the electrons accelerated during impulsive bursts must interact in dense regions ($>10^{11}$ cm^{-3}). This limit is still stronger ($>10^{13}$ cm^{-3}) if the rapid variability at energies >10 MeV is considered. The electron acceleration timescale can thus be as short as a few 100 ms for a few hundred keV electrons and of the order of 1 s for above 10 MeV electrons.

On the contrary, "long duration" events observed by PHEBUS above 100 keV (see, e.g., Fig. 4) do not show any evidence for time structures on timescales less than a few seconds even when the refined analysis is performed on the high time resolution mode recorded in the rising part of the event. The fastest fluctuations found are rather of the order of a few tens of seconds. The events consist generally of minute duration peaks superposed on a less intense and more slowly varying component (Talon et al. 1993a, b). The absence of fast time structures in these long-duration hard X-ray/gamma-ray events does not necessarily imply that the acceleration timescales are longer than in impulsive events. It may simply indicate that as was already suggested for many X-ray and gamma-ray events, the particles interact in a less dense region where their collisional lifetime is longer than the acceleration timescale (see, e.g., Vilmer 1987). This picture is consistent with the existence of two observed components with different temporal and spectral characteristics: a low-energy and more rapid component which could reflect partial particle precipitation in a dense region while the high-energy and more slowly varying component could result from some efficient trapping of higher energy particles in the acceleration/injection region (Talon et al. 1993b). This kind of behavior has been reported once for a

gradual event observed by *Hinotori*. The spatially resolved microwave observations give support to the previous hypothesis since the radio source is resolved into two components. One of them varies in time similarly to the lowest energy X-rays while the other one characterised by a weaker magnetic field reflects the higher energy time profiles (Kawabata et al. 1982; Nakajima 1983).

3.2. Coronal Signatures of the Accelerated Electrons: Evolution of Magnetic Structures in the Course of a Flare

Flare-accelerated electrons (a few tens to a few hundreds of keV) produce also radio emission in the corona through, for example, coherent plasma radiation in the metric-decimeter domain at a height ranging from 5×10^4 to 2×10^5 km above the photosphere. Many previous coordinated studies of hard X-ray and radio observations of solar flares have shown that hard X-ray and radio emissions arise from electrons produced by a common acceleration/injection (Raoult et al. 1985; Trottet 1986). While the hard X-ray measurements provide information about the particle numbers and spectra, the radio bursts are tracers of the large-scale magnetic structures in which electrons propagate from the acceleration volume toward the higher corona.

The study of the long-duration flare of 1990 May 15 at 13:04 UT (35 minutes at energies >60 keV) observed by PHEBUS and by the Nançay Multifrequency Radioheliograph in the decimeter-meter radio wave domain (Radioheliograph Group 1989) confirmed that close similarities are found between hard X-ray and radio emissions in a flare (Fig. 3 of Trottet et al. 1993b). Both emissions start within a few minutes and have similar durations. Previous detailed comparisons of the time histories of hard X-ray and decimeter/meter radio emissions had often led to the conclusion that apart from comparable durations there was not a one-to-one correspondence between both emissions, due to the specific dependence of the radio emissions on local conditions. However, the present study shows that there is a one-to-one correspondence between hard X-ray peaks and enhanced radio emissions, but that the posi-
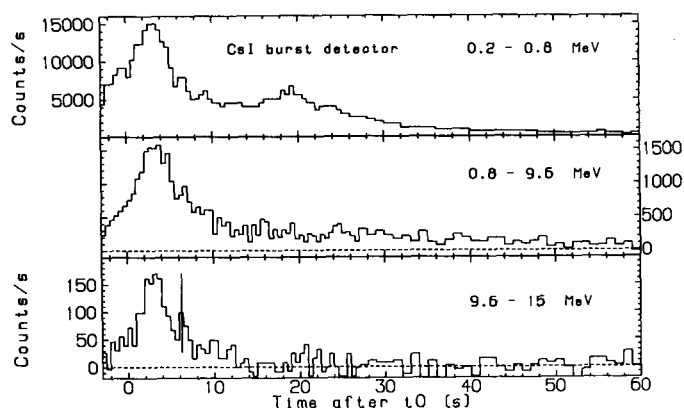

FIG. 3.—From Pelaez et al. 1992. Temporal evolution of the count rate observed by the SIGMA anticoincidence shield with an accumulation time of 0.5 s during the 1990 June 11 event. The 3 σ statistical error bar is indicated for the time structure above 10 MeV which is referred to in the text (t_0 = 09:43:35:842 UT).
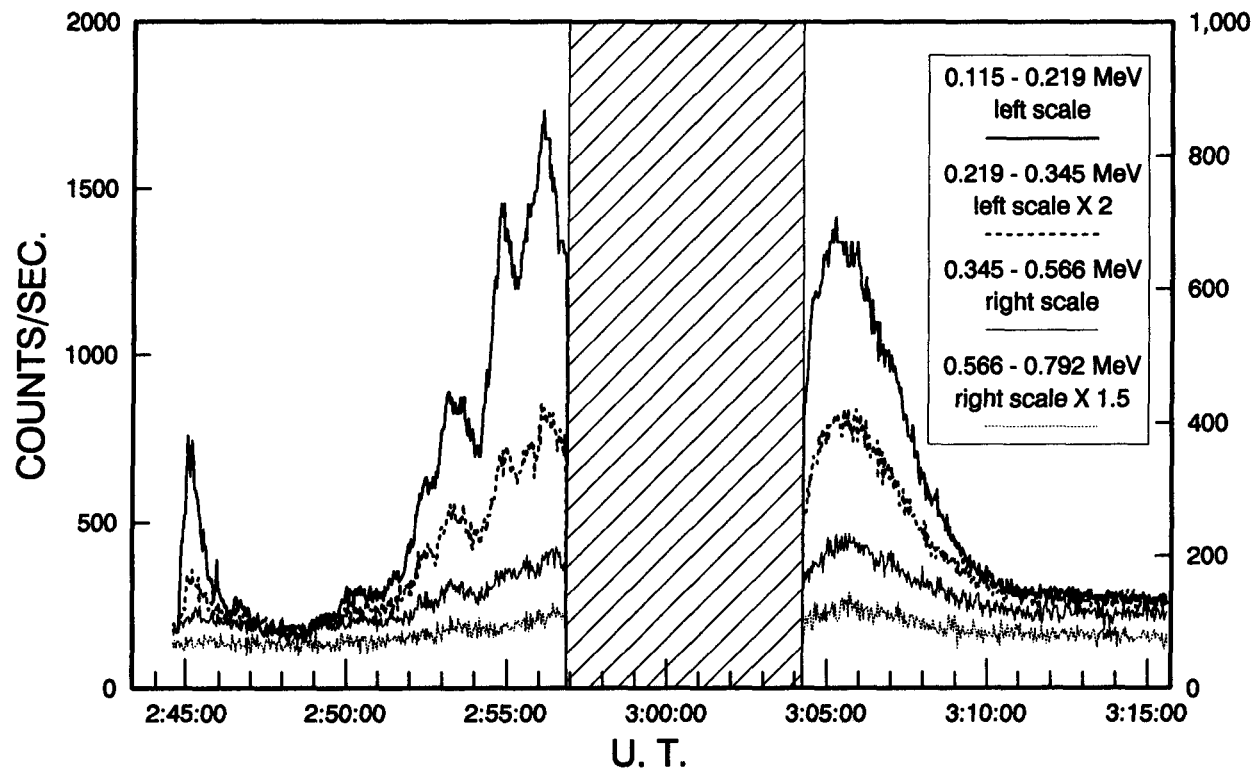
Fig. 4.—From Talon et al. 1993b. Temporal evolution of the count rate observed by PHEBUS in the burst mode with an accumulation time of 2 s during the 1990 April 15 event. The dashed area corresponds to a time interval where no burst data are available.

tion on the Sun, the spectral characteristics, and the sense of polarization of the radio-emitting sources vary from one hard X-ray peak to the other. As the delay between electron production (as revealed by the hard X-ray time profile) and the changes in the radio emission pattern is short compared to typical wave propagation times from the acceleration region (presumably located in the low corona [$n = 10^{10}-10^{11}$ cm^{-3}] as suggested by radio observations of electron beam radiations [see, e.g., Benz & Aschwanden 1991]) to the decimeter-meter emitting region, this suggests that electrons propagate in different magnetic structures during the different hard X-ray peaks. Particle drift across the magnetic field is not an efficient mechanism in a medium with density greater than 10^9 cm^{-3} typical of the acceleration region since energetic electrons diffuse at most a few meters before losing their energy through collisions (Achterberg & Kuijpers 1984). Furthermore, the more efficient diffusion across the magnetic field due to, for example, magnetic fluctuations becomes important only for large-amplitude fluctuations in a region of low density ($n < 10^8$ cm^{-3}) and for high-energy electrons (>100 keV) (Achterberg & Kuijpers 1984). Under these conditions, the rapid changes of the radio emission pattern are more in favor of rapid changes of the magnetic structure involved in the acceleration rather than to electron diffusion from a single acceleration site. This study performed on one flare is consistent with previous results (Machado et al. 1988; Willson et al. 1990) and is in agreement with the earlier idea that a hard X-ray flare is made of several elementary bursts (van Beek, de Feiter, & de Jager 1974). It

shows, however, that each elementary burst involves a slightly different site of the acceleration volume. Such observational results could be also used as an argument in favor of the fragmentation of the energy release (see the review by Benz in this issue).

Figure 5 shows the hard X-ray/gamma-ray and radio time profiles for the 1990 June 11 event. It is a high-energy (>10 MeV) impulsive event associated with an Hα 2B flare located close to the Sun's center at N10W22 (Pelaez et al. 1992; Talon et al. 1993b). No significant emission was detected in the flare above 40 MeV. This high-energy cutoff suggests that the >10 MeV continuum was produced by no pion decay radiation but predominantly ultrarelativistic electrons (see, e.g., Rieger & Marschhaüser 1990). The 10–40 MeV emission starts early in the event (at 09:43:20 UT.) confirming the rapid acceleration of electrons to energies >10 MeV at the onset of a flare. The radio emission shown in Figure 5 (Trottet et al. 1993b) comprises two components: (1) a noise storm emission observed at low frequencies which already existed before the onset of the hard X-ray/gamma-ray event; (2) an impulsive radio burst (type III/V) starting at 09:43:35 UT. The comparison of the different time profiles suggests that: (1) the rapid increase of the high-energy emission arises in close coincidence with the onset of the highest frequency radio emission; (2) at each frequency the radio emission switches on in association with a new hard X-ray/gamma-ray peak with different intensity and spectrum. The lack of radio signature at 327 and 435 MHz during the rising phase of the hard X-ray and gamma-ray emis-
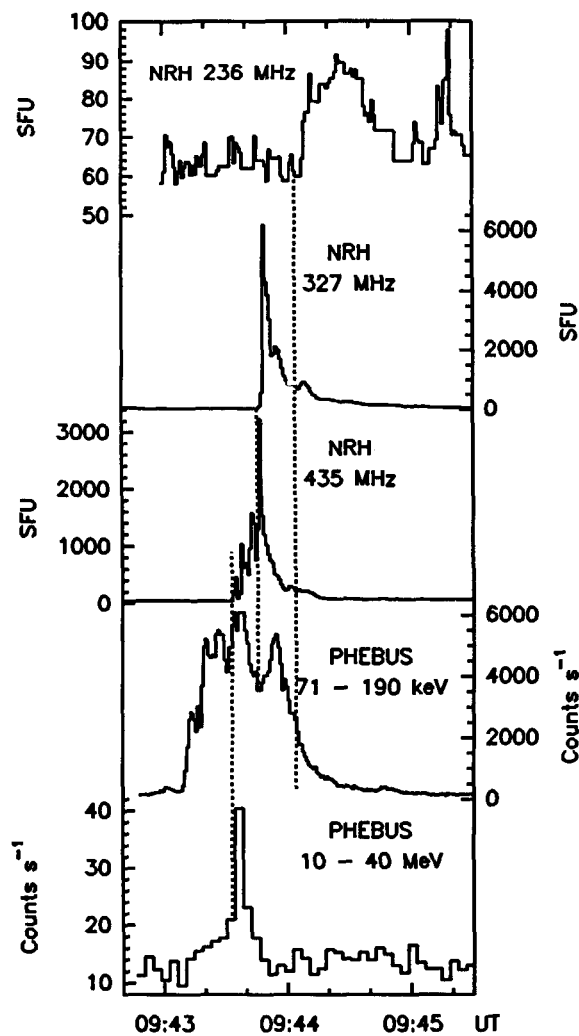
FIG. 5.—From Trottet et al. 1993b. Time histories of the 71–190 keV and 10–40 MeV count rates, and of the 435, 327, and 236 MHz radio flux density observed by the Nançay Multifrequency Radioheliograph for the 1990 June 11 event.

4. ULTRARELATIVISTIC ELECTRONS AND NONTHERMAL IONS IN SOLAR FLARES

4.1. Heliocentric Angle Distribution of High-Energy Emission

Since the beginning of the observations of high-energy events it has been noticed that there is a tendency of these emissions to be associated with flares at the limb (Rieger et al. 1983). This limb brightening was confirmed with the whole observations of cycle 21 (Vestrand et al. 1987; Rieger 1989; see Fig. 6). However, during the rise toward cycle 22, *SMM* measurements show several events that were located well on the disk (Vestrand et al. 1991; Fig. 6). The question whether cycle 22 behaves differently from cycle 21 is still open: (1) on one hand, Vestrand et al. (1991) show that the limb fraction of high-energy event observed by *SMM* (ratio of the number of flares with heliocentric angle such as $\sin \theta > 0.9$ to the total number) still shows a statistically significant excess compared to the production for isotropic radiation, in good consistency with the one observed for cycle 21; (2) on the other hand Ramaty & Mandzhavidze (1993) show that if the number of *SMM* events with $\sin^2 \theta > \frac{3}{4}$ is considered, then the hypothesis of isotropic emission in cycle 22 cannot be ruled out. Other high-energy events have been recently observed with SIGMA and PHEBUS on *GRANAT* (Pelaez et al. 1991, 1992; Talon et al. 1993b) as well as with GAMMA 1 (Akimov et al. 1991) and COMPTON (Kanbach et al. 1993). The fraction of disk events is also quite high among these flares (Fig. 6 and Table 2 of Mandzhavidze & Ramaty 1993), but in order to achieve an updated heliocentric angle distribution, it is necessary to inter-calibrate the different experiments so as to compare the relative fluxes. It is also necessary to distinguish the different com-
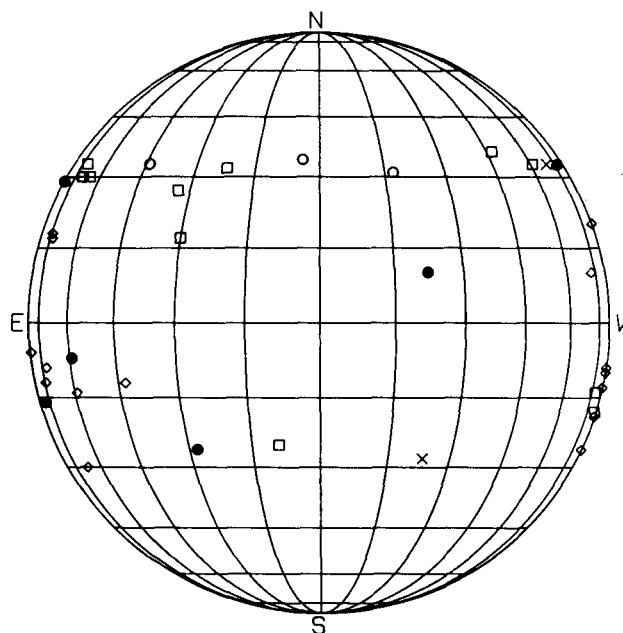
sions indicates that although energetic electrons are present in the chromosphere or low corona, they do not have access during that phase to the higher corona. The radio, X-ray, and gamma-ray evolutions observed during that event also indicate that electrons propagate and are produced in different magnetic structures during the different hard X-ray peaks and suggest furthermore that the number of accelerated particles and the hardness of their spectrum depend on physical conditions in the acceleration region.

The association between the rapid increase of the high-energy flux and the appearance of a new radio component in the corona was similarly reported for another high-energy disk event (Chupp et al. 1993). For that last event it was found moreover that there is a coincidence between the high-energy rapid enhancement and a new eruptive Hα feature (Chupp et al. 1993). Such a behavior had previously been reported for another disk flare (Wülzer, Canfield, & Rieger 1990). The picture that emerges from all these observations is that the radiation originates in a complex magnetic environment.

FIG. 6.—Positions of flares detected at energies >10 MeV by *SMM*-GRS during cycle 21 (*diamonds*) and cycle 22 (*squares*) (from Rieger 1989, and Vestrand et al. 1991), by SIGMA and PHEBUS (*filled circles*) (Pelaez et al. 1991; Talon et al. 1993b), GAMMA 1 (*cross signs*) (Akimov et al. 1991) and COMPTON (*open circles*) (Kanbach et al. 1993 and Table 2 from Mandzhavidze & Ramaty 1993).

ponents of the high-energy radiation (electron bremsstrahlung or pion decay radiation) since they present different anisotropies (MacKinnon & Brown 1989; Kocharov & Kovaltsov 1990; Ramaty et al. 1988; McTiernan & Petrosian 1991; Mandzhavidze & Ramaty 1992a). The analysis of the >10 MeV energy spectra has revealed the existence of pion decay radiation in a small number of events so far (six events) (Mandzhavidze & Ramaty 1993), suggesting that in most observed cases, the high-energy radiation arises from ultrarelativistic electrons. Apart from an electron anisotropic acceleration with a preferential direction tangential to the photosphere, this limb brightening can also result from the transport of initially isotropic electrons in a converging magnetic field, if this field is nearly normal to the photosphere (MacKinnon & Brown 1989; Kocharov & Kovaltsov 1990; Ramaty et al. 1988; McTiernan & Petrosian 1991). In such a context, the observations of some events close to the disk center (such as the 1990 June 11 event) could indicate that the electron bremsstrahlung arises from upward-moving electrons, probably reflected at mirror points below the transition region (Vestrand et al. 1991). The rapid variability observed at energies above 10 MeV (see § 3.1) could support this idea. An alternative possibility is that the magnetic field is not radial or that as suggested by the coordinated observations at other wavelengths, the emission comes from a complex magnetic environment. Apart from studying the statistical distribution of these high-energy events, it is thus also necessary to examine the magnetic environment in which they occur.

4.2. *1991 June 11 Event: Hardness of the Ion Spectrum*

This flare is one of the major flares produced by AR 6659 during its transit across the solar disk. Figure 7 (from Trottet et al. 1993a) shows the temporal evolution of the event as observed by PHEBUS (see also the COMPTEL observations by Ryan et al. 1993). In addition to bremsstrahlung emission, this flare produced strong nuclear lines (Fig. 8). The hard X-ray emission lasts for more than 10 minutes and presents well-defined peaks with durations of typically 1 minute (Fig. 7). No energy-dependent delays are observed in the peak times even with a 1 s accumulation time suggesting that during this main phase possible coronal trapping of energetic electrons does not substantially affect the hard X-ray time profiles which mostly reflect that of the acceleration (see, e.g., Vilmer 1987). The count rates of the excess produced by gamma-ray line emission (Fig. 7) have been determined for each time interval by extrapolation up to 10 MeV of the electron bremsstrahlung component observed below 1 MeV and subtraction of this component from the total count rate recorded in the 2.13–2.38 MeV and 4.2–7.3 MeV bands (Trottet et al. 1993a). The time history of the 4.2–7.3 MeV excess resulting from the interaction of 10–100 MeV nucleon^{-1} ions is very similar to that of hard
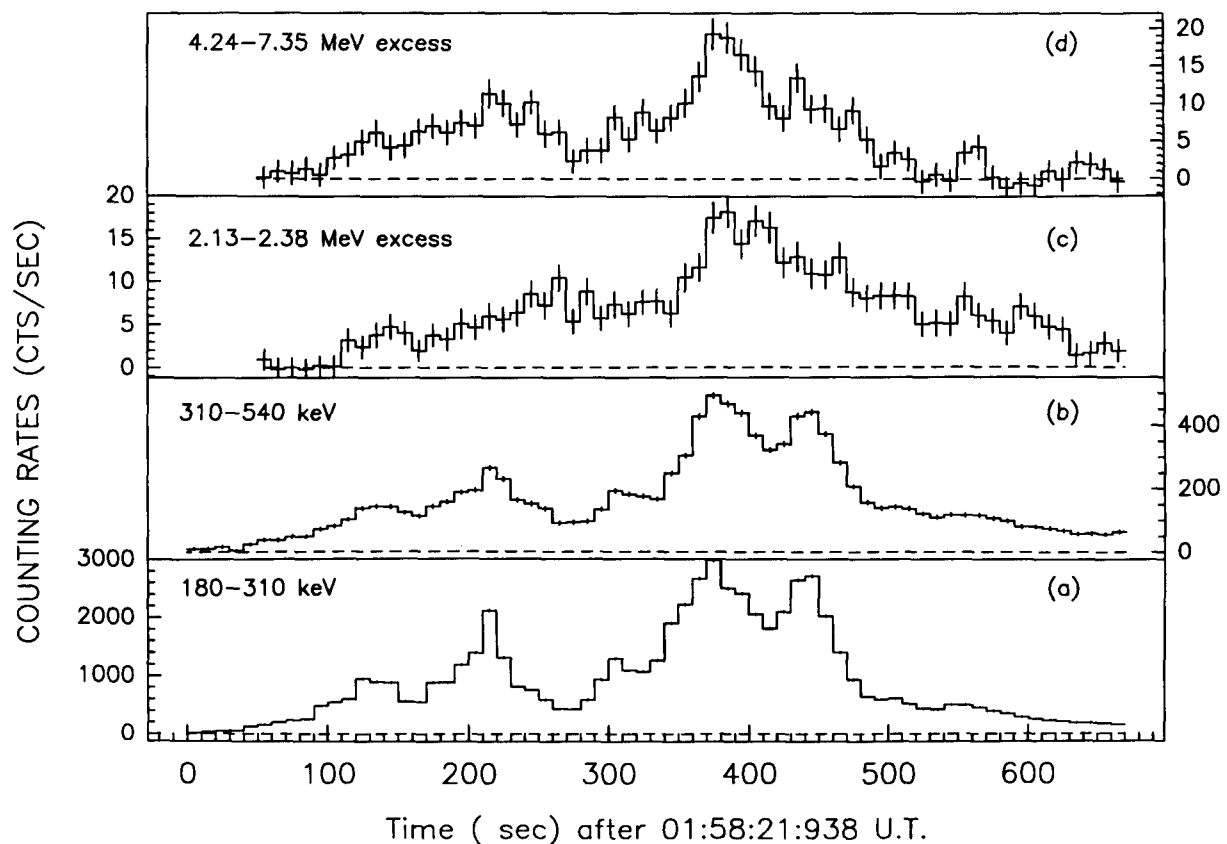

FIG. 7.—From Trottet et al. 1993a. Temporal evolutions of the 180–310 keV (*a*) and 310–540 keV (*b*) count rates, and of the 2.13–2.38 MeV excess (*c*) and 4.24–7.35 MeV excess (*d*) count rates for an accumulation time of 10 s observed by PHEBUS for the 1991 June 11 event.
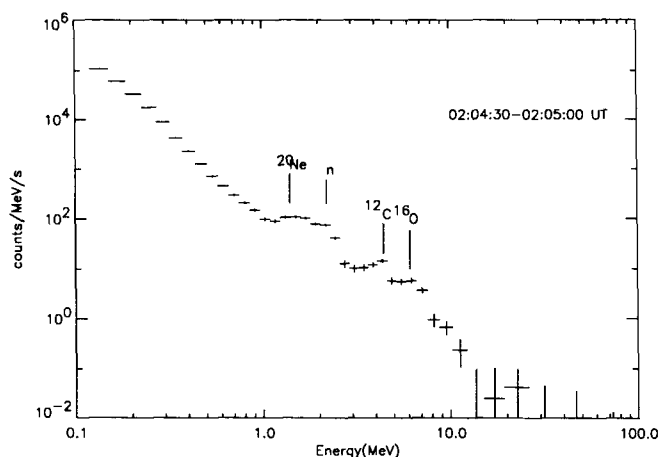
FIG. 8.—From C. Barat, private communication. Raw spectrum above background recorded by PHEBUS for the 1991 June 11 event.

X-ray (electron) emission. This suggests that electrons and ions are accelerated together on timescales less than a few tens of seconds and that there is no evidence of coronal trapping of energetic ions in this phase (Hulot, Vilmer, & Trottet 1989). The 2.13–2.38 MeV excess was shown to be a good measurement of the delayed 2.223 MeV line resulting from the radiative capture of thermalized neutrons on ambient hydrogen (Trottet et al. 1993a). This excess exhibits peaks which are smoother than those in the 4.2–7.3 MeV band and decays more slowly than this band. In addition to radiative capture on ^{1}H, thermal neutrons experience nonradiative capture on ^{3}He (e.g., Wang & Ramaty 1974), and the time dependence of the 2.223 MeV line provides a measurement of the abundance ratio $r = {}^3$He/H in the interaction region (Wang & Ramaty 1974; Prince et al. 1983). Assuming that the neutron production rate follows the prompt 4.2–7.3 MeV flux and that the neutron capture arises in a medium with the usually assumed hydrogen density of 1.3×10^{17} cm^{-3} (Prince et al. 1983; Hua & Lingenfelter 1987b), we determine r of the order of 3×10^{-5} ($2 \times 10^{-5} < r < 5 \times 10^{-5}$) from the fit of the 2.13–2.38 MeV excess time profile. This value is in good agreement with previous estimations (Chupp et al. 1981; Hua & Lingenfelter 1987b). If the time-integrated 2.13–2.38 MeV and 4.2–7.3 MeV excess count rates are considered as good approximations of the total fluences in, respectively, the delayed and the prompt lines, their ratio gives a determination of the hardness of the proton spectrum. Using calculations performed by Hua & Lingenfelter (1987a) for $r = 2 \ 10^{-5}$, we find the spectrum represented by either a Bessel function with $\alpha T = 0.02$ or a power law with a spectral index of 3.5, in the case of an isotropic ion distribution. These values are in the same range as those generally obtained for gamma-ray line flares (Hua & Lingenfelter 1987a; Ramaty et al. 1993). The PHEBUS observations did not show any significant flux at energies above 10 MeV, probably because of a high background at the vicinity of the satellite. However, the EGRET detector revealed the existence of a long-duration component at GeV energies lasting for more than 8 hr after the main phase (Kanbach et al. 1993). It was shown by Mandzhavidze & Ramaty (1992b) that the high-energy spectrum in this late phase as well as the temporal decay

of the >50 MeV flux can be explained by the radiation of ions (and in a lesser extent of electrons which decay faster) accelerated during the main flare phase and subsequently trapped in magnetic loops. The temporal decay of the nuclear lines observed by OSSE (Murphy et al. 1993) give support to this interpretation. It is worthy to note that the value of the spectral index of the proton spectrum deduced by the fluence ratio of the de-excitation and 2.223 MeV lines measured with PHEBUS during the main phase and the value deduced through the modeling of the pion emission decay are the same ($s = 3.5$), suggesting that in this flare the proton spectrum can be described with a single power law from ~ 10 MeV to at least 5 GeV (Ramaty & Mandzhavidze 1993). A further study is necessary, however, to understand the link between the main phase in which most of the energetic particles precipitate and interact in dense layers and the late phase in which the emission is produced by partially trapped energetic particles.

4.3. 1990 May 24 Event

The PHEBUS and SIGMA experiments aboard GRANAT observed a long-duration high-energy (>10 MeV) event which occurred on 1990 May 24 in association with a limb flare (N33 W78), where GeV protons were observed in interplanetary space and the largest increase due to solar neutrons was recorded at ground levels (Pelaez et al. 1992; Talon et al. 1993b). Figure 9a displays the event time profile in several energy bands as observed by PHEBUS (Talon et al. 1993b). The hard X-ray event is so intense that the detectors are saturated below 843 keV. The detailed behavior of the time profiles between 0.8 and 10 MeV is discussed in Pelaez et al. (1992). Figure 9a shows that the flux increases rapidly at 20:47:40 UT in the whole 0.843–109.5 MeV band. The high-energy count rate displayed in Figure 9b shows that essentially two peaks are present at high energies (20:48:15 UT and 20:48:27 UT). While the intensity of the first peak is higher in the 15.9–21.2 MeV range, the two peaks are comparable in the 57.5–79.5 MeV range, and the second one dominates in the 79.5–110 MeV band. The evolution of the count rate above 60 MeV would be consistent with emission from pion decay radiation (Talon et al. 1993b). However, a more detailed study of the energy spectrum is necessary to determine the magnitude of this component. As in the case of the 1982 June 3 event (see Chupp 1990b for a review of the observations of this flare), the 1990 May 24 event presented a long high-energy tail after 20:50 UT lasting at least for 6 minutes until the end of the PHEBUS observations. In addition to pion decay radiation, this tail could also be partially produced by the arrival of escaping solar neutrons on the detector. Indeed, neutron detection at ground level shows a maximum between 20:50 and 20:55 UT (Pyle, Shea, & Smart 1991; Shea, Smart, & Pyle 1992) in rough coincidence with an enhancement between 20:50 and 20:52 UT in the count rate measured by PHEBUS above 57.5 MeV. If the bulk of the neutrons is produced at the time of the second hardest >10 MeV peak, the first neutrons arriving at the satellite have an energy of 600 MeV. This suggests that GeV ions have been accelerated during this flare. The striking feature is that the spectrum measured during the most intense part of the event in the 1–15 MeV range (between 20:47:55 and 20:48:35 UT) does not show any evidence of a clear excess in the nuclear
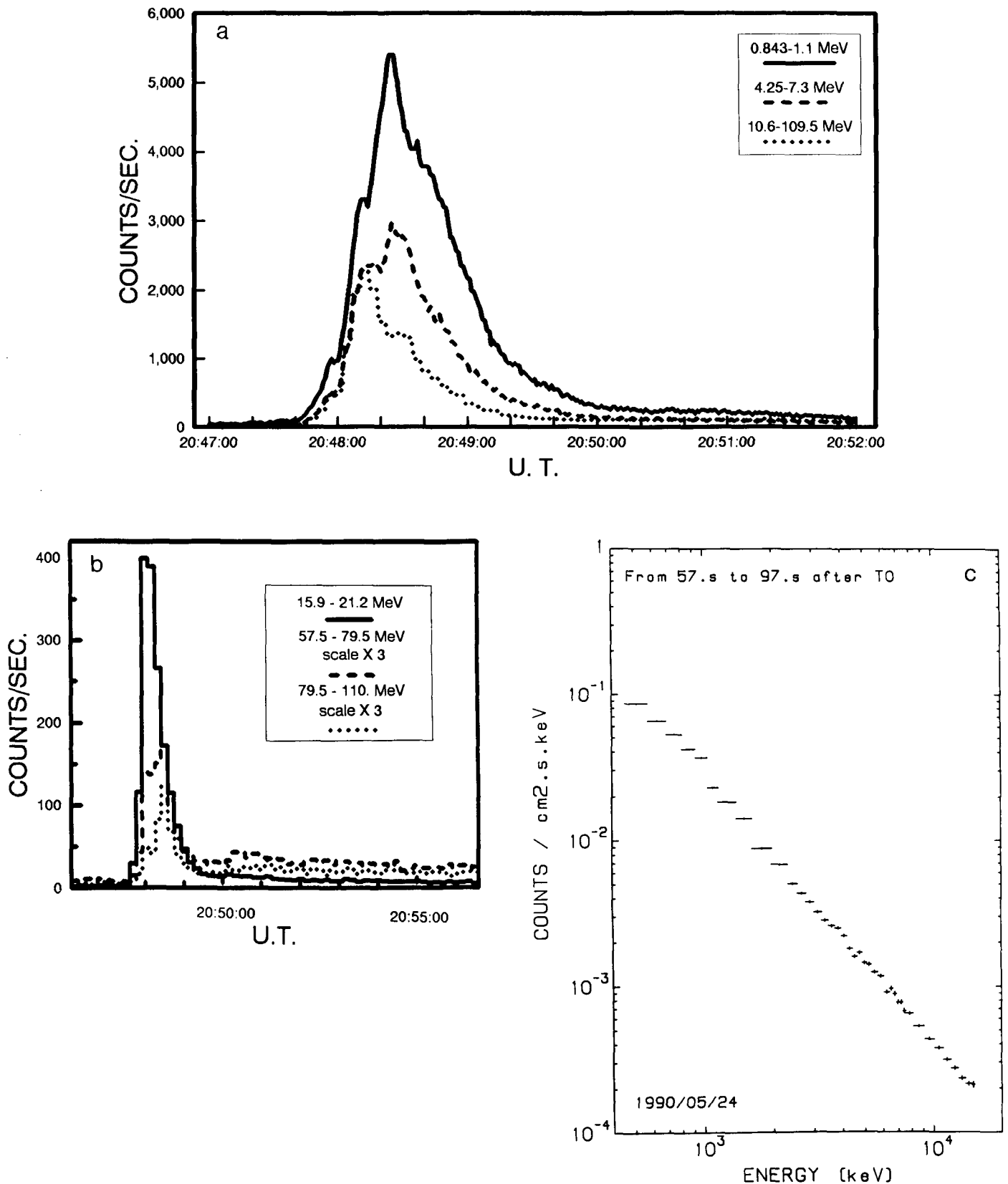
FIG. 9.—Adapted from Talon et al. 1993b and Pelaez et al. 1992. (a) Temporal evolution of the 0.843–1.1 MeV, 4.25–7.3 MeV, and 10.6–109.5 MeV count rate observed by PHEBUS for the 1990 May 24 event. The accumulation time is 1 s for the two lowest energy bands and 4 s for the highest one. (b) Temporal evolution of the 15.9–21.2 MeV, 57.5–79.5 MeV, and 79.5–109.5 MeV count rate observed by PHEBUS with an accumulation time of 12s. (c) Raw spectrum above background observed by the SIGMA CsI burst detector. The accumulation time goes from 20:47:55 to 20:48:35 UT (T0 = 20:46:58 UT).

gamma-ray line domain (Fig. 9c and Pelaez et al. 1992). The observations of the delayed 2.223 MeV line in the late phase of the flare (after 20:50 UT) reported by Terekhov et al. (1993) suggest, however, that in addition to high-energy escaping neutrons, this flare produced neutrons penetrating deep enough in the solar photosphere to give rise to the delayed radiative capture line. A more comprehensive study is necessary to understand the absence of detectable prompt gamma-ray lines in the most intense part of the flare.

5. DISCUSSION AND CONCLUSIONS

In this paper we have reviewed some results obtained with the hard X-ray and gamma-ray observations of the PHEBUS detectors and of the SIGMA anticoincidence shield aboard GRANAT. Special emphasis has been given to the constraints deduced on particle acceleration during solar flares. These observations represent the only solar high-energy data set in 1990 and the beginning of 1991 and thus allows us to provide some continuous coverage of solar activity at high energies. Even if the experiments operate with a burst mode, more than 100 solar bursts have been detected above 100 keV in 2.5 yr. Furthermore, a continuous coverage of long-duration events is obtained in some cases by the combination of the observations of the two experiments.

We have confirmed with these observations that there is a rapid acceleration of electrons (up to a few tens of MeV) at the beginning of a flare. The PHEBUS observations of "impulsive" bursts (duration less than 5 minutes at 100 keV) have provided strong constraints on the electron acceleration timescale: in short-duration events it is of the order of a few hundreds of milliseconds above 100 keV and of the order of 1 s for >10 MeV electrons. The COMPTON measurements confirm these findings. The observations also confirm the interaction of electrons in the dense region for short-duration events ($n > 10^{11}$ cm^{-3}). This limit is even stronger if the rapid variability at energies >10 MeV is considered ($>10^{13}$ cm^{-3}). On the other hand, longer characteristic timescales are observed for long-duration events, suggesting either a slower acceleration process or particle interaction in a less dense medium.

Special emphasis has been given to the signature of particle acceleration at radio wavelengths. It was shown that, during different hard X-ray subpeaks, electrons have access to different coronal magnetic structures. These modifications are so rapid that they also suggest changes in the magnetic structures involved in the acceleration. The magnetic environment of a high-energy disk flare dominated by electron bremsstrahlung has also been investigated. As previously reported for another event, it is shown that the rapid increase of the high-energy emission occurs in close coincidence with the appearance of a new radio source in the corona. Conversely, the onsets of new radio sources at lower and lower frequencies are associated with other hard X-ray/gamma-ray subpeaks with different intensities and spectra. Multiple magnetic structures are thus suggested in the development of the flare, and the number of accelerated particles as well as their energy spectrum seem to depend on physical conditions in the structures where the acceleration occurs.

New high-energy (>10 MeV) events have been detected with the spectrometers aboard GRANAT. Some of these events are associated with disk flares raising some questions about the heliocentric angle distributions of these flares and about the differences which may exist between the distributions observed in the previous and present activity cycle. The observations of some of the largest solar flares of the present cycle have been summarized in this review. The accelerated proton spectrum has been determined for the 1991 June 11 event from the ratio of line fluences. The long-duration event of 1990 May 24 is found to show similar characteristics to the largest flare observed by *SMM* during the previous cycle. The observations show a possible indication of pion radiation and the possible detection of neutrons at the satellite.

REFERENCES

Achterberg, A., & Kuijpers, J. 1984, A&A, 130, 111
Akimov, V. V., & GAMMA1 Team. 1991, in Proc. 22d Internat. Cosmic-Ray Conf. (Dublin), SH 2.3–6, 73
Barat, C., et al. 1988, in Nuclear Spectroscopy of Astrophysical Sources, ed. G. H. Share & N. Gehrels (New York: AIP), 395
Benz, A. O., & Aschwanden, M. J. 1991, in Lecture Notes in Physics 399, Eruptive Solar Flares, ed. Z. Svestka, B. V. Jackson, & M. E. Machado (New York: Springer), 363
Bruggmann, G., Vilmer, N., Klein, K. L., & Kane, S. R. 1993, Sol. Phys., in press
Chupp, E. L. 1982, in Gamma-Ray Transients and Related Phenomena, ed. R. E. Lingenfelter, H. S. Hudson, & D. M. Worall (New York: AIP), 363
———— 1988, Sol. Phys., 118, 137
———— 1990a, Science, 250, 229
———— 1990b, ApJS, 73, 213
Chupp, E. L., Forrest, D. J., Higbie, P. R., Suri, A. N., Tsai, C., & Dunphy, P. P. 1973, Nature, 241, 33
Chupp, E. L., et al. 1981, ApJ, 244, L171

Chupp, E. L., Trottet, G., Marschhaüser, H., Pick, M., Soru-Escaut, I., Rieger, E., & Dunphy, P. P. 1993, A&A, 275, 602
Dennis, B. R. 1988, Sol. Phys., 118, 49
Desai, U. D., et al. 1987, ApJ, 319, 567
Forrest, D. J., Vestrand, W. T., Chupp, E. L., Rieger, E., Cooper, J., & Share, G. H. 1985, in Proc. 19th Internat. Cosmic-Ray Conf. (La Jolla) (NASA CP-2376), 4, 146
Golonetskii, S. V., et al. 1991, Soviet Astron. Lett, 17, 83
Heristchi, D. J. 1986, ApJ, 311, 474
Hua, X. M., & Lingenfelter, R. E. 1987a, Sol. Phys., 107, 351
———— 1987b, ApJ, 319, 555
Hulot, E., Vilmer, N., & Trottet, G. 1989, A&A, 213, 383
Hurley, K., Niel, M., Talon, R., Estulin, I., & Dolidze, V. C. 1983, ApJ, 265, 1076
Kanbach, G., et al. 1993, A&AS, 97, 349
Kane, S. R., Chupp, E. L., Forrest, G. H., Share, G. H., & Rieger, E. 1986, ApJ, 300, L95
Kawabata, K., et al. 1982, in Proc. Hinotori Symp. on Solar Flares (Institute of Space and Astronautical Science), 168

Kiplinger, A. L., Dennis, B. R., Emslie, A. G., Frost, K. G., & Orwig, L. E. 1983, ApJ, 265, L99

Kocharov, L. G., & Kovaltsov, G. A. 1990, Sol. Phys., 125, 67

Leikov, N. G., et al. 1993, A&AS, 97, 345

Machado, M. E., Emslie, A. G., Fishman G. J., Meegan, G., Wilson, R., & Pachiesas, W. 1993, Adv. Space Res. (COSPAR), 13, 175

Machado, M. E., Moore, R. L., Hernandez, A., Rovira, M. G., Hagyard, M. J., & Smith, J. B. 1988, ApJ, 326, 425

MacKinnon, A. L., & Brown, J. C. 1989, A&A, 215, 371

Mandzhavidze, N., & Ramaty, R. 1992a, ApJ, 389, 739

—— 1992b, ApJ, 396, L111

—— 1993, Nucl. Phys., in press

McTiernan, J. M., & Petrosian, V. 1991, ApJ, 379, 381

Murphy, R. J., et al. 1993, in Proc. Compton Symp., in press

Nakajima, H. 1983, Sol. Phys., 86, 427

Pelaez, F., et al. 1992, Sol. Phys., 140, 121

Pelaez, F., et al. 1991, in 22d Internat. Cosmic-Ray Conf. Proc., SH2.3-11, 89

Prince, T. A., Forrest, D. J., Chupp, E. L., Kanbach, G., & Share, G. H. 1983, in 18th Internat. Cosmic-Ray Conf. Proc., 4, 79

Pyle, K. R., Shea, M. A., & Smart, D. F. 1991, in 22d Internat. Cosmic-Ray Proc., SH2.2-7, 57

Radioheliograph Group 1989, Sol. Phys., 120, 193

Ramaty, R., & Mandzhavidze, N. 1993, in Proc. Compton Symp., in press

Ramaty, R., Mandzhavidze, N., Kozlovsky, B., & Skibo, J. 1993, Adv. Space Res. (COSPAR), in press

Ramaty, R., Miller, J. A., Hua, X. M., & Lingenfelter, R. E. 1988, in Nuclear Spectroscopy of Astrophysical Sources, ed. G. H. Share & N. Gehrels (New York: AIP), 217

Ramaty, R., & Murphy, R. 1987, Space Science Rev., 45, 213

Raoult, A., Pick, M., Dennis, B. R., & Kane, S. R. 1985, ApJ, 299, 1027

Rieger, E. 1989, Sol. Phys., 121, 323

—— 1990, in Gamma-Ray Line Astrophysics Conf. Proc., ed. P. Durouchoux & N. Prantzos (New York: AIP), 421

Rieger, E., & Marschhaüser, H. 1990, in Proc. 3d MAX'91/SMM Workshop on Solar Flares: Observations and Theory, ed. R. M. Winglee & A. L. Kiplinger (Boulder: Univ. Colorado Press), 68

Rieger, E., Reppin, C., Kanbach, G., Forrest, D. J., Chupp, E. L., & Share, G. H. 1983, in Proc. 18th Internat. Cosmic-Ray Conf. (Paris), 10, 338

Ryan, J., et al. 1993, in Proc. Compton Symp., in press

Shea, M. A., Smart, D. F., & Pyle, K. R. 1992, Geophys. Res. Lett., 18, 1655

Talon, R., Barat, C., Dezalay, J. P., Vilmer, N., Trottet, G., Sunyaev, R., Terekhov, O., & Kuznetsov, A. 1993a, Adv. Space Res. (COSPAR), 13, 171

Talon, R., Trottet, G., Vilmer, N., Barat, C., Dezalay, J. P., Sunyaev, R., Terekhov, O., & Kuznetsov, A. 1993b, Sol. Phys., 147, 137

Talon, R., Vedrenne, G., Melioransky, A. S., Pissarenko, N, Shamolin, V. F., & Likin, O. B. 1975, in IAU Symp. 68, Solar Gamma-, X-, and EUV Radiation, ed. S. R. Kane (Dordrecht: Reidel), 315

Terekhov, O. V., et al. 1993, COSPAR abstracts E3-5, 5.10

Trottet, G. 1986, Sol. Phys., 104, 145

Trottet, G., Vilmer, N., Barat, C., Dezalay, J. P., Talon, R., Sunyaev, R., Kuznetsov, A., & Terekhov, O. 1993a, A&AS, 97, 337

Trottet, G., Vilmer, N., Barat, C., Dezalay, J. P., Talon, R., Sunyaev, R., Terekhov, O., & Kuznetsov, A. 1993b, Adv. Space Res. (COSPAR), 13, 285

Van Beek, H. F., de Feiter, L. D., & de Jager, C. 1974, Space Res., 14, 477

Vestrand, W. T., Forrest, D. J., Chupp, E. L., Rieger, E., & Share, G. H. 1987, ApJ, 322, 1010

Vestrand, W. T., Forrest, D. J., & Rieger, E. 1991, in Proc. 22d Internat. Cosmic-Ray Conf. (Dublin), SH2.3-5, 69

Vilmer, N. 1987, Sol. Phys., 111, 207

Wang, H. T., & Ramaty, R. 1974, Sol. Phys., 36, 129

Willson, R. F., Klein, K. L., Kerdraon, A., Lang, K. R., & Trottet, G. 1990, ApJ, 357, 662

Wu, S. T., et al. 1986, in Energetic Phenomena on the Sun, ed. M. Kundu & B. Woodgate (NASA CP-2439), 5-1

Wülzer, J. P., Canfield, R. C., & Rieger, E. 1990, in Proc. 3d MAX'91/SMM Workshop on Solar Flares: Observations and Theory, ed. R. M. Winglee & A. L. Kiplinger (Boulder: Univ. Colorado Press), 149

Yoshimori, M. 1989, Space Sci. Rev., 51, 85

Yoshimori, M., Takai, Y., Morimoto, K., Suga, K., & Ohki, K. 1992, PASJ, 44, L107